ADVANCED FUNCTIONAL MATERIALS
www.afm-journal.de

Self-Replenishing Dual Structured Superhydrophobic Coatings Prepared by Drop-Casting of an All-In-One Dispersion

A. C. C. Esteves, Y. Luo, M. W. P. van de Put, C. C. M. Carcouët, and G. de With**

Robust dual structured superhydrophobic coatings which replenish spontaneously their surface chemical composition on new multi-scale structured surfaces, recreated upon damage, are described. The surface repair occurs at room temperature, via intrinsic elements of the coatings, all covalently bonded. These coatings can be prepared from all-in-one dispersions by a simple drop-cast method, with different thicknesses and on various substrates. The critical factors to optimize the self-replenishment are described and three main design principles are postulated. The superhydrofobicity of the coatings is maintained even after 500 abrasion cycles. The principles reported can be extended towards self-healing other surface-dependent functionalities, that is, anti-bacteria, anti-fouling, or drag-reduction, which will maintain high performance levels all through their life-cycle with low cost and energy demand for maintenance and surface repair.

1. Introduction

Biodiversity in nature resulted from millions of years of evolutionary processes through which materials with different structures and morphologies were developed.[1] For plants, the key of survival and expansion was the multifunctional boundary (plants cuticle) which provides specific surface properties such as radiation, protection, controlled wettability, temperature control, or anti-adhesive properties.[1,2] Functional coatings have very much in common with this boundary structure, as they are meant to protect the under layers and provide specific interactions with the surrounding environment, for instance, controlled wettability, response to temperature or light stimulus, anti-fouling, or self-cleaning properties.[2,3] It is then no wonder that nature examples, like the waxy and structured surface of the Lotus leaves,[4] have been the natural source of inspiration for functional surfaces which rely on well-defined surface chemistry and topography,[5] for example, superhydrophobic coatings.

However, most of the functional surfaces currently available can be easily damaged by routine use, resulting in the immediate loss of the chemical functionalities, surface–structure and related chemical/physical properties. This irreversible loss reduces the materials service-life time and increases the energy and costs involved in maintenance and repair. Hence, the investigation of robust structured-surfaces, which are able to withstand daily usage for a longer period of time, is critical for the sustainable development of advanced materials. Although many efforts have been made towards durable and robust functional surfaces,[6–8] damage and wear will always be unavoidable. Thus, a preferable approach is the introduction of self-repairing mechanisms[9,10] to prevent early failure or lowering of the materials performance along their life-time.

Many mechanisms and strategies have been reported for recovering mechanical properties and bulk damage;[11–13] however, only a few focus on the recovery of surface properties or functionality, in particular when they also depend on the topography.[14,15] One of the most promising approaches recently investigated consists of the repair of the surface chemistry on regenerated topographies.[14,16] Li et al.[17], for instance, prepared superhydrophobic porous polymer coatings by a chemical vapour deposition (CVD) method, which recover low surface energy components on damaged surfaces, upon adsorption of water and via the migration of fluoro-alkylsilanes previously impregnated. In fact, the few self-healing strategies reported for surface-functionalities rely on desorption or migration of low surface energy components previously adsorbed/deposited by CVD on porous materials into the damage loci. Moreover, in the majority of the cases a triggering stimulus, such as temperature or moisture, is required to initiate the healing, as recently pointed out in a review by Xue and Ma.[6]

In this work, we report robust superhydrophobic coatings which recover spontaneously their surface chemical composition on new structured-surfaces, self-recreated upon damage (**Scheme 1**). These coatings are prepared from an all-in-one dispersion by a simple drop-cast method. For these systems, the surface repair occurs at room temperature, using intrinsic elements of the coatings, all covalently bonded, which affords a very robust film. The current work reveals the way to design a new generation of self-healing functional coatings which are accessible through typical coating processing methods, with different thicknesses, on various substrates.

Dr. A. C. C. Esteves, Y. Luo, M. W. P. van de Put, C. C. M. Carcouët, Prof. G. de With
Laboratory of Materials and Interface Chemistry
Eindhoven University of Technology
PO Box 513, 5600 MB, Eindhoven, The Netherlands
E-mail: a.c.c.esteves@tue.nl; G.deWith@tue.nl

DOI: 10.1002/adfm.201301909

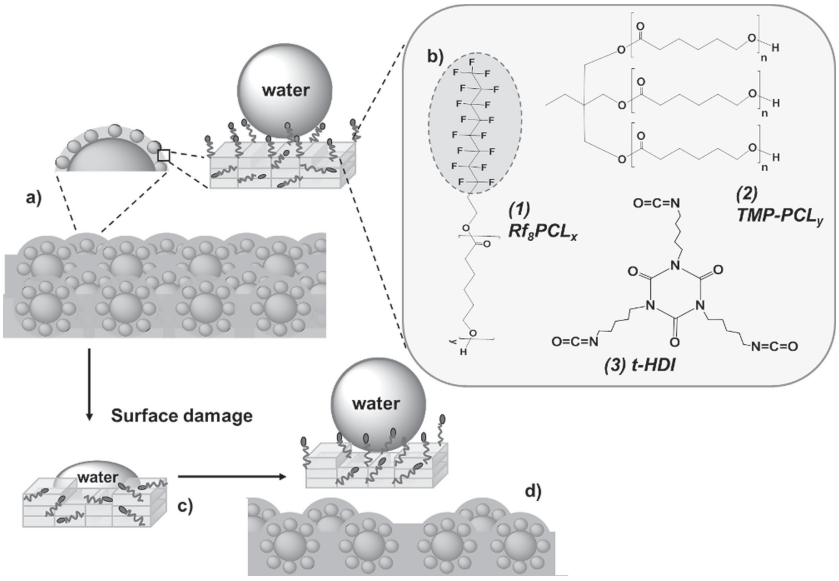

Scheme 1. Self-replenishing of surface-structured superhydrophobic coatings: a) dual-structure obtained with dual-size silica nanoparticles; b) chemical components of the cross-linked polymer network, 1) perfluorinated-dangling chains (Rf8PCL*x*; *x* = CL units), 2) poly(caprolactone) precursor (TMP-PCL*y*, *y* = 3*x* CL units), and 3) tri-isocyanate cross-linker (t-HDI); c) damaged surface; and d) recovered chemical composition at the new topographic surface, created by the damage.

2. Results and Discussion

The preparation of the dual-structured coatings took in consideration our previous findings on polymeric self-replenishing coatings,[18] and three main design principles were put forward: 1) to chemically bond all the components providing a robust coating and avoid leaching of the self-healing elements, 2) to maintain sufficient low surface energy dangling chains at the surface but also in the bulk, allowing repetitive replenishing events, and 3) to distribute homogeneously sufficient nanoparticles in the bulk-network, for topography recreation. The dual-scale topography was built via chemically bonded silica nanoparticles of two different sizes to a cross-linked polymer network[18] (Scheme 1a). The low surface energy was provided by fluoroalkyl-terminated polymeric dangling chains, tethered to the cross-linked polymer network (Scheme 1b, 1). When the surface is damaged, the particles homogeneously dispersed in the bulk provide a new topography. Driven by differences of energy between the new surfaces and the bulk, the dangling chains of the polymer layer embedding the particles, spontaneously re-orient towards the new air interfaces, recovering the surface chemical composition (see Scheme 1a–c).

The SiO_2 nanoparticles used were synthesized within two size ranges $\bar{D}_1 \approx 700$ nm and $\bar{D}_2 \approx 70$ nm, as measured by dynamic light scattering (DLS). The larger particles were modified with amino-propyltriethoxysilane (APTES) to provide a better adhesion between particles and polymer. The amino and hydroxyl surface groups were used for chemical bonding via reaction with a tri-isocyanate cross-linker (Scheme 1b, 3), forming urea or urethane bonds, respectively. The cross-linked network consisted of a hydroxyl-terminated poly(caprolactone) precursor with controlled degree of polymerization (DP = 24) (Scheme 1, 2) which was reacted with the isocyanate cross-linker, at moderate temperatures and short time periods (see the Experimental Section for details). The low surface energy was achieved via the fluorine-terminated dangling chains containing a hydroxyl-terminated poly(caprolactone) spacer, also reacted with the cross-linker (Scheme 1, 1).

2.1. Dual-Scale Structured Coatings

An all-in-one dispersion containing the dual-size SiO_2 nanoparticles, the polymers and the cross-linker was prepared in *N*-Methyl Pyrrolidone (NMP) with a determined solid content (75 total wt% of SiO_2 in relation to the total solid content). The components have by nature distinct properties: hydrophobic (fluorinated-segment) versus hydrophilic (silica particles and caprolactone segments). To promote the homogenous distribution of all the components, several pre-cross-linking steps of the particles and polymer components were performed (see Experimental Section). The final dispersion was directly drop-casted on clean glass substrates and thermally treated for 60 min at 80 °C for cross-linking (typical thickness targeted ≈150 μm).

To tune the surface chemical composition and topography, several dual-structured coatings were investigated. Reference coatings without nanoparticles were also prepared and characterized (see **Table 1**).

The morphology of the coatings was first investigated by scanning electron microscopy (SEM). In all the coatings the dual-size nanoparticles were homogeneously distributed through the bulk (**Figure 1**a) and also organized on a protuberant layer at the air-interface, in a raspberry-like morphology (Figure 1b and inset). The topography of the coatings was further evaluated by atomic force microscopy (AFM) which clearly showed a dual-scale roughness on the micrometer and nanometer range (**Figure 2**a).

The surface chemical composition was investigated by X-ray photoelectron spectroscopy (XPS) (Figure 2b). For all the coatings,

Table 1. Description and characterization of the coatings prepared with dual size nanoparticles DLS average diameter, $\bar{D}_1 \approx 700$ nm and $\bar{D}_2 \approx 70$ nm), and with Rf_8PCL_{16} dangling chains, before intentional surface damage.

Coating with raspberry dual-size ($\bar{D}_1$ and $\bar{D}_2$) SiO_2 nanoparticles (75 wt%)[a]	Overall wt% Fluorine*	Water CA_{adv} [°] ± 2	Water CA hysteresis [°] ± 2
DC0	0	73	15
DC0.65	0.65	151	13
DC1	1	147	9
DC1.5	1.5	136	21
DC2	2	137	23

[a]In relation to the total amount of solid contents.

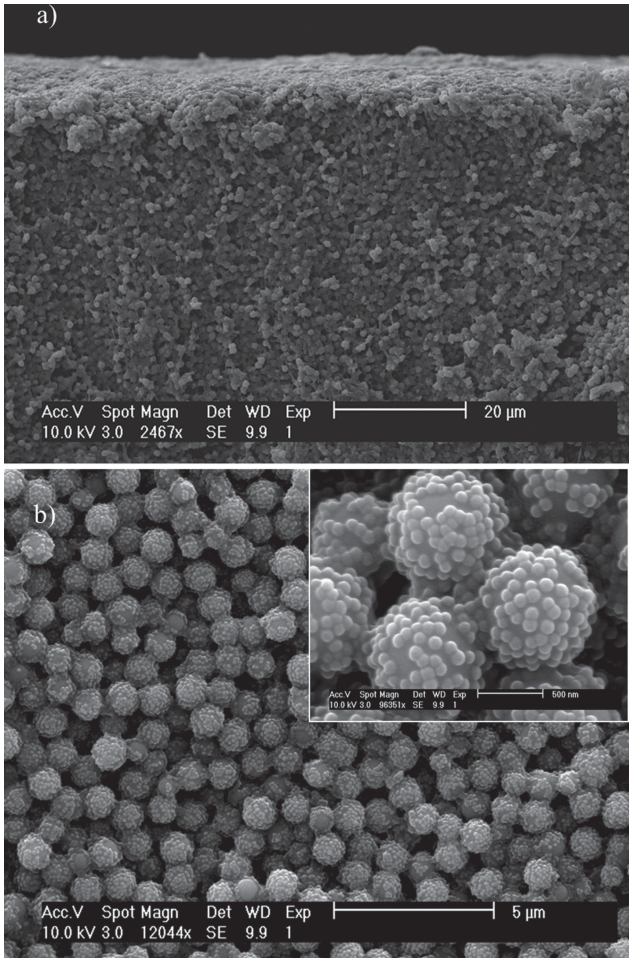

Figure 1. SEM images of typical dual-structured coatings with raspberry-like morphology at the air-interface: a) cross-section (detail of the top 60 µm of an ≈150 µm thick coating) and b) air-interface (inset: higher magnification showing the raspberry-like morphology).

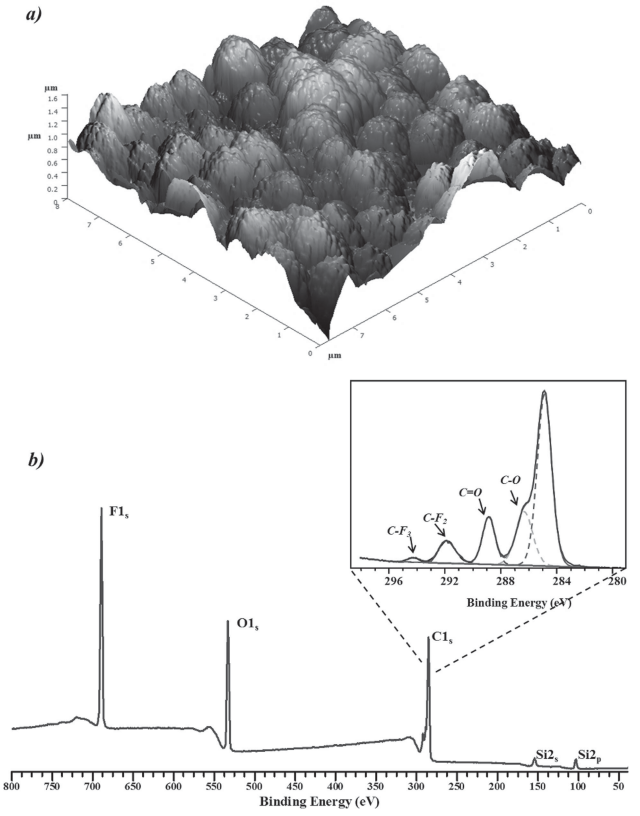

Figure 2. Topography and surface chemical composition of typical dual-structured coatings with raspberry-like morphology at the air-interface: a) AFM 3D height image and b) XPS spectrum (inset: detailed C1s XPS spectrum).

atomic O1s, C1s, Si2p, and F1s were present at the surface.[19] Furthermore, by the deconvolution of the C1s peak five carbons with different environments (Figure 1d, inset) where identified: CF_3 (294.3 eV), CF_2 (291.8 eV), C=O (288.9 eV), C–O (286.3 eV) and C–C/C–CH (284.8 eV).[19] These combined results provide a clear confirmation of the presence of silica nanoparticles and fluoroalkyl-dangling chains at the top 10 nm layer of the coating, respectively (surface probed with a take-off angle of 0°).

The concentration of the fluorinated species and the presence of a polymeric spacer in the dangling chains are critical parameters for the self-replenishing effect.[18,20] In the current system, the presence of nanoparticles and extra interfaces during the cross-linking could possibly impart spatial restriction to the movement of the components, influencing the wettability or the self-replenishing behavior. Hence, coatings made with polymeric spacers of different chain length (DP from 8 to 22) and an overall wt% of F ranging from 0.65 to 2 were investigated by static and dynamic water contact angles (CA).

As for the fluorinated-dangling chains length, an optimum was found while using a polymeric spacer of 16 caprolactone (CL) units (Rf_8PCL_{16}) on coatings with 0.65 wt% of F (**Figure 3**a). These results are in agreement with previous experimental-simulation studies on polymer coatings,[18,20] where the optimum found for the CA was attributed to the most favorable positioning/orientation of the fluorinated-dangling chains at the first air-interface.

For coatings prepared with the smallest wt% of F (0.65 wt% of F in total solid content corresponds to an equivalent of 2.5 wt% of F in a coating without particles), the dynamic water CA of the initial surfaces were already in the superhydrophobic range (Figure 3b). At higher concentrations, no significant increase was observed. In fact, a small decrease of the CA_{adv} was registered, indicating a possible entrapment of the fluorinated-dangling chains in the bulk of the coating. The CA hysteresis at the first air-interface formed is however, relatively high (20–25°) for all the coatings, indicating that they are rather closer to the high adhesive superhydrophobic regime, as described by Jiang and co-workers.[21]. The importance of the dual-scale hierarchical roughness to achieve the stable Cassie-Baxter superhydrophobic state has been largely discussed,[22] and the permanent entrapment of air into the asperities has been identified as a critical factor.[23] In our coatings, the high CA hysteresis is most likely the result of two possible effects: 1) poor ability to entrap air into the nanometer-scale roughness which leads to pinning of the water film into the raspberry-like structures;[24,25] and 2) rapid rearrangement of the hydrophilic caprolactone segments upon contact with water, as previously reported by us[20] and others.[26]

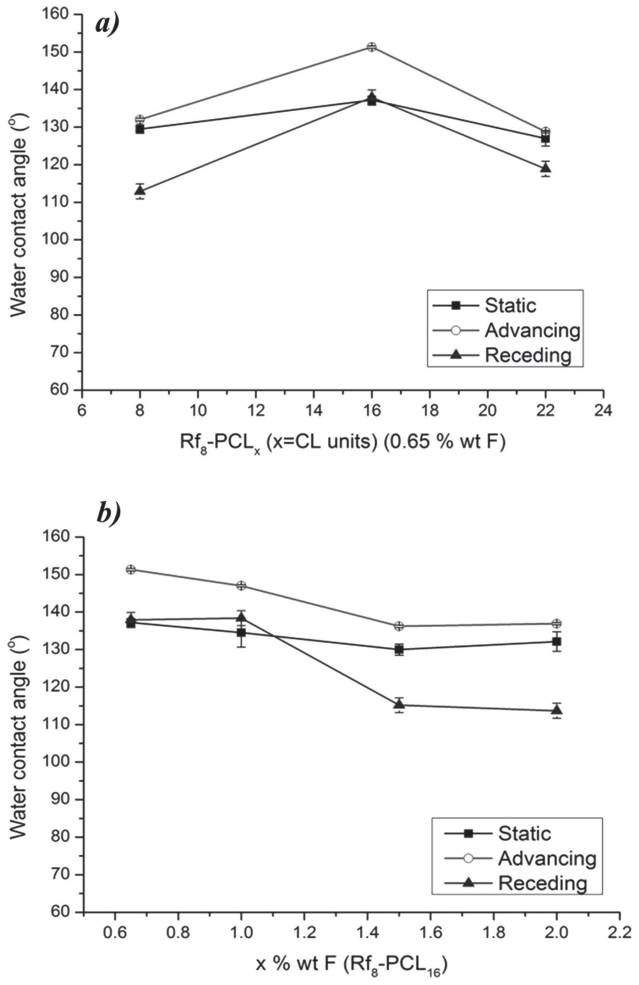

Figure 3. Static and dynamic water contact angles on dual-structured coatings: a) effect of the length (DP – number of CL units) of the polymeric spacer of the fluorinated-dangling chains (on coatings with 0.65 wt% F) and b) effect of different fluorine concentration (wt% of F, using Rf_8-PCL_{16} dangling chains).

The use of raspberry-like particles for superhydrophobic surfaces has been previously described, mostly via controlled deposition on substrates.[27,28] However, the majority of these surfaces is very prone to damage and a further coating/embedding with a low surface energy component was always required to achieve a high water CA. Hence, it remains remarkable that the coatings we report here achieve such high water CA from a thick layer prepared directly from an all-in-one dispersion. Moreover, depending on the thickness required, the dispersion can be applied homogeneously by drop-casting (up to a few hundreds of μm) or spin-coating (a few tens of μm) either on glass, aluminium, or polycarbonate substrates.

2.2. Robustness and Self-Replenishing of the Dual-Scale Surface Structured Coatings

In practical applications, these coatings will be inevitably damaged by accidental scratches, dirt rubbing, or prolonged contact with chemicals. The premature leaching of particles or fluorinated-dangling chains would jeopardize the self-healing ability. Hence, the coatings chemical and mechanical resistance was firstly investigated. For this purpose, the coatings were submitted to extraction procedures in different solvents (water, chloroform, and ethanol) combined with short sonication periods, after which they were dried under vacuum and characterized. SEM revealed that after these experiments the nanoparticles were still embedded in the polymer bulk (Supporting Information, Figure SI–1a). The weight loss registered by gravimetry was very low: 0.1 (water), 2.5 (ethanol), and 4.3 (chloroform) wt% of the initial coating. The solvent fractions were dried and the solid residues were analyzed by ^{1}H NMR. The chemical shifts were assigned to poly(caprolactone) fragments (Supporting Information, Figure SI–1b). No chemical shifts related to the fluorinated-dangling chains were found. Hence, even after harsh extraction in different solvents, only a small solid residue was extracted from the coatings consisting mainly of free polymer fragments. This robustness was the first evidence of success of our first design principle: to chemically bond all the coatings components, avoiding leaching of nanoparticles and/or fluorinated chains.

To study the self-replenishing of the structured-coatings, we mimicked the damage that occurs on real applications by abrasion (testing set-up described in the Supporting Information, Figure SI–2). The coatings with different wt% of F and raspberry-like structures were initially submitted to 50 abrasion cycles (400 grit sandpaper under constant pressure of 4300 Pa) (**Figure 4**a). The coatings with lower wt% of F showed a sharp decrease of the water CA after 10 cycles, and decreased further to hydrophilic values (<70°) after 50 cycles. However, for coatings with higher wt% of F the CA were less affected and even increased for the highest concentrations (≥1.5 wt%). The structured-coatings with 1.5 wt% of F were further submitted to 500 abrasion cycles (in total a ≈90 μm layer was removed) (Figure 4b). Regardless of the harsh damage imposed on the surface, the water CA remained high and it should be noticed that the CAH decreased considerably (≈10°). Although the concentration of the fluorinated dangling chains did not seem to be critical for the water CA of the initial structured-surface (Figure 3a), it was evidently determinant for the self-replenishment. The enrichment of the initial air-interface with low surface energy groups may occur naturally during the cross-linking process, driven by energy differences between the surface and bulk.[18] However, for repetitive replenishment, a sufficient concentration (in this case, ≥1.5 wt% F) of the dangling chains in the bulk cross-linked network is required (i.e., existence of a reservoir), as postulated on our second design principle.

The morphology of the coatings before and after 500 abrasion cycles was investigated by SEM. Large scale (macroscopic) roughness profiles were induced by abrasion (**Figure 5**b) and new layers of large and small particles were exposed at the air-interface, creating a new micro- and nanometer level roughness (Figure 5d,f). To infer on the influence of the macroscopic roughness introduced by the abrasion test, coatings prepared with equivalent wt% of F but without particles were tested (**Figure 6**a). After 500 abrasion cycles, these coatings maintain relatively constant water CA values, showing that the effect of the macroscopic roughness on the surface wettability can be disregarded.

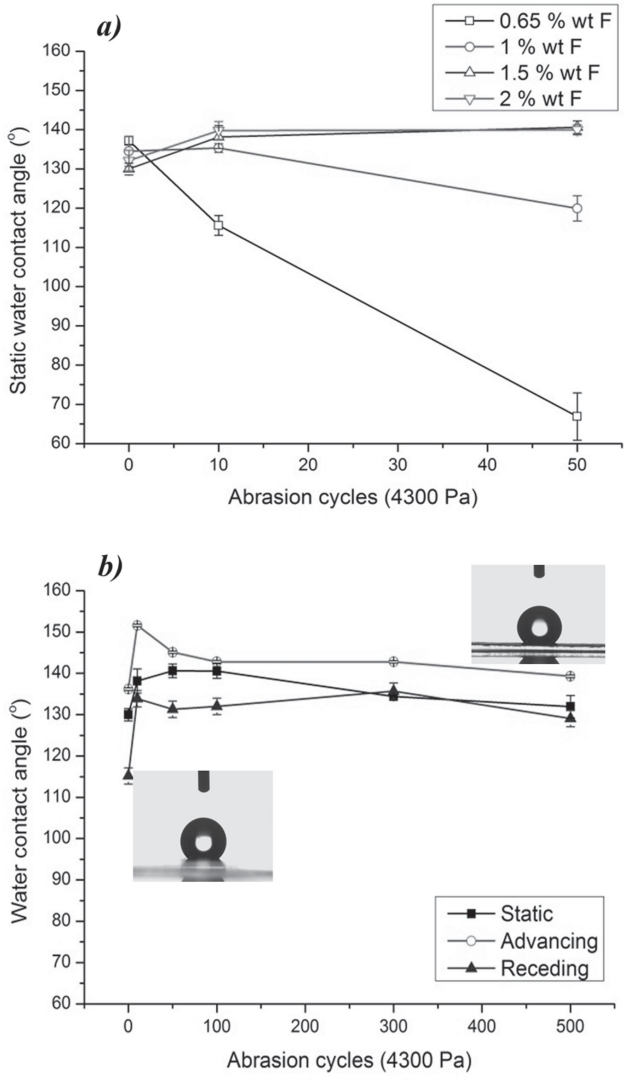

Figure 4. Static water contact angles of dual-structured coatings after abrasion cycles with sand paper (400 grit and a constant pressure of 4300 Pa): a) 50 cycles on coatings with different wt% of F, using Rf_8-PCL_{16} dangling chains and b) 500 cycles on coatings with 1.5 wt% of F and Rf_8-PCL_{16} dangling chains.

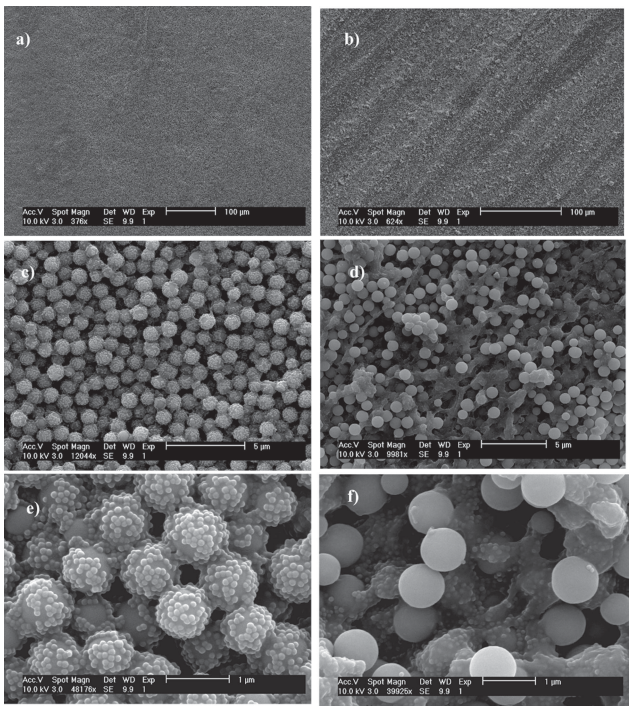

Figure 5. SEM images of dual-structured coatings at different magnifications: a,c,e) before and b,d,f) after 500 abrasion cycles with sand paper of 400 grit and under a constant pressure of 4300 Pa.

Even if the regenerated topography did not show the initial raspberry morphology, it seems to be efficient on entrapping sufficient air into the surface–structure to maintain a high water CA. These results show the importance of our third design principle; that is, to have sufficient topography-inducing elements (particles) homogeneously distributed in the bulk, so that they can re-create topographies upon repetitive damage. In this case, the recreation of a multi-scale surface roughness may even be beneficial for the surface wettability, as also reported by others.[29]

XPS analyses of the structured-coatings after 500 abrasion cycles indicates that the F/C atomic ratio on the top 10 nm layer increases slightly in relation to the initial surface (Figure 6b), while the Si/C atomic ratio is rather similar. These results provide further evidence of the re-orientation of the dangling chains, covalently bonded to the polymer layer involving the regenerated topography (assuming the possible cross-contamination from the abrasion procedure insignificant; see Supporting Information for experimental details). Hence, the self-replenishing effect we observed for the structured-coatings is most likely a combined result of the regenerated multi-scale topography and the re-orientation of the fluorinated dangling chains at the new air-interfaces.

3. Conclusions

Robust superhydrophobic coatings which can replenish the surface chemical composition on new multi-scale topographies created by the damage were prepared, from an all-in-one dispersion and using a simple drop cast method. Three main design principles have been postulated and proven. The fine tuning of the coatings conditions, such as concentration and mobility of the low surface energy component, and concentration and distribution of the topography-inducing elements, are critical factors to optimize the self-replenishment. The principles reported can be extended to other self-healing surface-dependent functionalities, that is, anti-bacteria, anti-(bio)fouling, or drag-reduction, with high performance levels through their life-cycle and low cost and energy demand for maintenance and surface repair.

4. Experimental Section

Materials and Equipment: Tetraethyl orthosilicate (TEOS, 99%), 3-Amino-propyltriethoxysilane (APTES, 98%) both purchased from

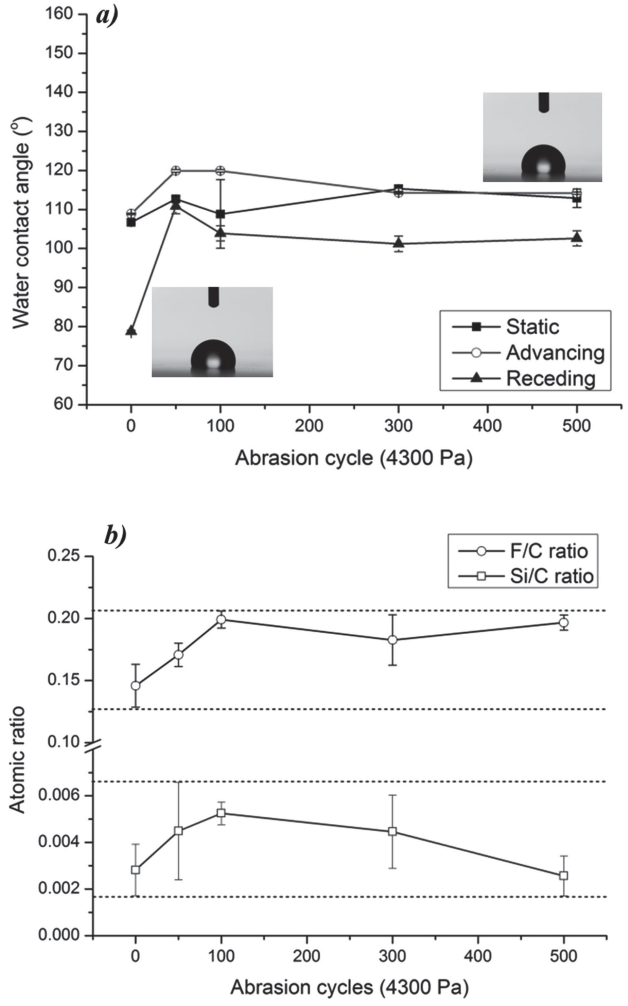

Figure 6. Characterization of the coatings: effect of abrasion cycles on a) the static and dynamic water contact angle of coatings without nanoparticles and b) the F/C and Si/C ratio of the dual-structured coatings. For the abrasion tests, sand paper of 400 grit and was used with a 4300 Pa constant pressure.

Merck (Honenbrunn, Germany) and 25% ammonia aqueous solution from Merck (Darmstadt, Germany), were used as received. Compounds 1 and 2 in Scheme 1, were prepared as described by Dikić et al.[30]. The cross-linker (compound 3) further referred as t-HDI, was obtained from Perstop as tolonate HDT-LV2, which consists mainly of hexamethylene diisocyanate trimer (equivalent weight of NCO EW_{NCO} = 183 g; NCO functionality = 2.8, molar mass = 504.6 g/mole). Isopropanol, ethanol, and *N*-Methyl pyrrolidone (NMP) were obtained from Biosolve (Valkenswaard, the Netherlands). All solvents and chemicals were used without any further purification, unless stated otherwise.

DLS was performed on a Malvern Zetasizer Nano ZS Instruments, using distilled water or ethanol as dispersing media. A Philips XL-30 ESEM FIB microscope was used for SEM analyses. For the preparation of the coatings, a Laurell WS-650-23NPP-LITE Spin Coater was employed. CA measurements were performed on a Dataphyscis OCA 30 with ultrapure water as probe liquid. AFM measurements were performed on a SMENA-B Solver P47HT scanning probe microscope with a gold-coated NSG 03 tip from NT-MDT. XPS was carried with a K-Alpha, ThermoScientific spectrometer using an aluminum anode (Al Kα = 1486.3 eV) operating at 510 W with a background pressure of ≈2×10^{-8} mbar. The spectra were recorded using the VGX900 data system collecting an average of 60 scans. All carbon C1s peaks corresponding to hydrocarbons were calibrated at a binding energy of 284.5 eV, to correct for the energy shift caused by charging. The spectra were acquired at take-off angle of 0° relative to the surface normal, corresponding to a probe depth of ≈10 nm. The fluorine-to-carbon (F/C) ratio was determined from curves fitted to the C1s spectra, according to different carbon environment (C–C, C–H, C–O, C–N, C=O, C–F_2, and C–F_3). The F/C and Si/C ratio were estimated from the corresponding area ratios by the following equations:

$$F/C = \frac{[A(CF_2).2 + A(CF_3).3]}{A(CF_2) + A(CF_3) + A(C=O) + A(C-O) + A(C-C)} \quad (1)$$

$$Si/C = \frac{[A(Si)]}{A(CF_2) + A(CF_3) + A(C=O) + A(C-O) + A(C-C)} \quad (2)$$

Preparation of Silica Nanoparticles with 700 nm ($\bar{D}_1$)According to the Stöber Method:[31] An initial reaction mixture was prepared by adding 21 mL of a 25% aqueous ammonia solution to a mixture of 75 mL isopropanol and 25 mL methanol, which was stirred at 300 rpm to achieve a homogeneous dispersion. Next, 10 mL TEOS was added drop-wise in about 10 minutes. The white suspension formed was kept stirring for about five hours at room temperature. After this reaction time, the white particles were separated by centrifugation (20 min, at 8000 rpm) and re-precipitated three times in a 50% ethanol/water solution (using similar centrifugation conditions). The particles separated from the supernatant (white solid) were vacuum-dried at 60 °C for 16 h.

Preparation of Silica Nanoparticles with 70 nm ($\bar{D}_2$) According to the Stöber Method:[31] The initial reaction mixture was prepared in a 250 mL round bottom flask, where 15 mL of a 25% aqueous ammonia solution was firstly added to 200 mL of ethanol. The mixture was stirred at 400 rpm to guarantee a homogeneous dispersion. Next, 6 mL of TEOS was added drop-wise at 60 °C in about 10 min. The white suspension formed was kept stirring for about five hours at 60 °C. After this reaction time, the particles were separated by centrifugation (30 min, at 15000 rpm), re-precipitated 3 times in 50% ethanol/water solutions and separated (using similar centrifugation conditions). The particles separated from the supernatant (white solid) were vacuum-dried at 60 °C for 16 h.

Amino-Modification of Silica Particles: 1 g of 700 nm silica particles ($\bar{D}_1$) were re-dispersed into 100 mL ethanol. The mixture was sonicated for 15 min to guarantee that the silica particles were homogeneously dispersed. Subsequently, 0.1430 g APTES in 10 mL ethanol was added drop-wise to the silica suspension. The suspension was stirred (300 rpm) at 50 °C under nitrogen atmosphere for about 24 h. After this reaction time, the particles were separated by centrifugation and washed three times with ethanol (20 min, at 8000 rpm). The collected particles (white solid) were vacuum-dried at 50 °C for 16 h.

Pre-Cross-Linking of the Precursors: First, 0.029 g of $\bar{D}_2$ silica nanoparticles were dispersed in 0.155 g of NMP by sonication during 90 min. Second, 0.050 g of a 30 wt% t-HDI solution (in NMP) was added to a mixture of 0.186 g TMP-PCL_{24} in 0.931 g NMP. The mixture was magnetically stirred during 90 minutes at 75 °C. Next, 0.190 g of pre-cross-linked TMP-PCL_{24}/t-HDI/NMP mixture and 0.104 g of the amino-modified $\bar{D}_1$ particles were added to the initial $\bar{D}_2$ suspension in NMP. The total suspension was sonicated for 15 min. Next, 0.009 g of Rf_8-PCL_{16} was added and sonicated for another 15 min. Finally, 0.036 g of a 30 wt% t-HDI solution (in NMP) was added. The total molar ratio of NCO/(OH or NH) was kept at 1.2 to ensure the full conversion of OH or NH groups.

Preparation of Dual-Size Coatings by Drop-Casting: The all-in-one dispersion was drop-casted on clean glass slides (20 mm × 20 mm) until they were completely wet. The film was cured for 60 min at 80 °C under vacuum. The typical thickness of the coatings obtained with this process was about 70 to 150 µm, depending on the drop-casting volume of coating suspension and coated area.

Supporting Information

Supporting Information is available from the Wiley Online Library or from the author.

Acknowledgements

Ing. Marco Hendrix and Ing. Nick Lousberg are acknowledged for support with AFM and SEM, respectively. The authors thank Prof. R.A.T.M. van Benthem and Ing. L.G.J. van der Ven for helpful discussions and Agentschap NL, IOP-Self-healing (#SHM01053) for financial support.

Received: June 4, 2013
Published online: September 12, 2013

[1] K. Koch, B. Bhushan, W. Barthlott, *Soft Matter* **2008**, *4*, 1943.
[2] F. Xia, L. Jiang, *Adv. Mater.* **2008**, *20*, 2842.
[3] B. Bhushan, Y. C. Junga, *Prog. Mat. Sci.* **2011**, *56*, 1.
[4] J. Wang, H. Chen, T. Sui, A. Li, D. Chen, *Plant Sci.* **2009**, *176*, 687.
[5] L. C. Gao, T. J. McCarthy, *Langmuir* **2006**, *22*, 2966.
[6] C. H. Xue, J. Z. Ma, *J. Mater. Chem. A* **2013**, *1*, 4146.
[7] J. Genzer, K. Efimenko, *Science* **2000**, *290*, 2130.
[8] I. A. Larmour, G. C. Saunders, S. E. J. Bell, *Appl. Mater. Interfaces* **2010**, *2*, 2703.
[9] D. Y. Wu, S. Meure, D. Solomon, *Prog. Polym. Sci.* **2008**, *33*, 479.
[10] M. D. Hager, P. Greil, C. Leyens, S. van der Zwaag, U. S. Schubert, *Adv. Mater.* **2010**, *22*, 5424.
[11] M. M. Caruso, D. A. Davis, Q. Shen, S. A. Odom, N. R. Sottos, S. R. White, J. S. Moore, *Chem. Rev.* **2009**, *109*, 5755.
[12] Y. L. Chen, A. M. Kushner, G. A. Williams, Z. B. Guan, *Nat. Chem.* **2012**, *4*, 467.
[13] M. M. Caruso, B. J. Blaiszik, S. R. White, N. R. Sottos, J. S. Moore, *Adv. Funct. Mater.* **2008**, *18*, 1898.
[14] H. Jin, X. L. Tian, O. Ikkala, R. H. A. Ras, *ACS Appl. Mater. Interfaces* **2013**, *5*, 485.
[15] T. S. Wong, S. H. Kang, S. K. Y. Tang, E. J. Smythe, B. D. Hatton, A. Grinthal, J. Aizenberg, *Nature* **2011**, *477*, 443.
[16] H. Zhou, H. X. Wang, H. T. Niu, A. Gestos, T. Lin, *Adv. Funct. Mater.* **2013**, *23*, 1664.
[17] Y. Li, L. Li, J. Sun, *Angew. Chem. Int. Ed.* **2010**, *49*, 6129.
[18] T. Dikić, W. Ming, R. A. T. M. van Benthem, A. C. C. Esteves, G. de With, *Adv. Mater.* **2012**, *24*, 3701.
[19] J. F. Moulder, W. F. Stickle, P. E. Sobol, K. D. Bomben, *Handbook of X-Ray Photoelectron Spectroscopy*, Perkin-Elmer Corporation, Minnesota, USA.
[20] A. C. C. Esteves, K. Lyakhova, L. G. J. van der Ven, R. A. T. M. van Benthem, G. de With, *Macromolecules* **2013**, *46*, 1993.
[21] L. Feng, Y. Zhang, J. Xi, Y. Zhu, N. Wang, F. Xia, L. Jiang, *Langmuir* **2008**, *8*, 4114.
[22] M. Nosonovsky, B. Bhushan, *Micro. Eng.* **2007**, *84*, 382.
[23] A. Lafuma, D. Quéré, *Nat. Mater.* **2003**, *2*, 457.
[24] K. L. Cho, A. H. F. Wu, I. I. Liaw, D. Cookson, R. N. Lamb, *J. Phys. Chem. C* **2012**, *116*, 26810.
[25] H. Teisala, M. Tuominen, M. Aromaa, M. Stepien, J. M. Makela, J. J. Saarinen, M. Toivakka, J. Kuusipalo, *Langmuir* **2012**, *28*, 3138.
[26] J. T. Koberstein, *J. Polym. Sci., Polym. Phys.* **2004**, *42*, 2942.
[27] W. Ming, D. Wu, R. A. T. M. van Benthem, G. de With, *Nano Lett.* **2005**, *5*, 2298.
[28] Z. Qian, Z. Zhan, L. Song, H. Liu, *J. Mater. Chem.* **2009**, *19*, 1297.
[29] E. Bittoun, A. Marmur, *Langmuir* **2012**, *28*, 13933.
[30] T. Dikić, W. Ming, P. C. Thüne, R. A. T. M. van Benthem, G. de With, *J. Polym. Sci., Polym. Chem.* **2008**, *46*, 218.
[31] W. Stöber, A. Fink, E. Bohn, *J. Colloid Interface Sci.* **1968**, *26*, 62.